ELSEVIER

Nuclear Physics A734 (2004) 536–540

NUCLEAR PHYSICS A

www.elsevier.com/locate/npe

Analysis of momentum distributions of projectile fragmentation products

O.Tarasov [1,2,*]

[1] *National Superconducting Cyclotron Laboratory, Michigan State University, East Lansing, MI 48824-1321, USA*
[2] *Flerov Laboratory of Nuclear Reactions, Joint Institute for Nuclear Research, Dubna, Moscow region, 141980, Russia*

Abstract

A model describing fragment momentum distributions as a function of the projectile energy has been developed. This model called "Universal parameterization" is based on the convolution between a gaussian distribution corresponding to Goldhaber model of fragmentation and an exponential attenuation arising from friction between projectile spectator and participant. An analysis of several experimental data sets has been performed to obtain the coefficients of the Universal Parameterization in order to avoid drawbacks inherent to the fragmentation statistical model. The Universal parameterization is incorporated in the LISE++ code for fragment transmission calculations.

1. Introduction

Fragment momentum distributions measured in relativistic heavy ion collisions are typically observed to be gaussian shaped where the center of distribution corresponds to the projectile velocity. Within the framework of the independent particle model [1], it was shown that the parabolic dependence of the width $\sigma_{||}$ of the gaussian shape describing the parallel momentum distribution can be described by:

$$\sigma_{||}^2 = \sigma_0^2 \, A_F (A_P - A_F)/(A_F - 1), \tag{1}$$

where A_F is the fragment mass, A_P is the projectile mass, and σ_0 is the reduced width related to the Fermi momentum (approximately equal to 90 MeV/c).

However, this model is unable to account for the following features:

- The anomalously small values of σ_0 observed at lower energies;
- The differences in widths associated with nuclides of the same mass;
- The reduction of the velocity relation between fragment and projectile at low energies;
- The occurrence of an exponential tail in fragment momentum distributions in reactions at low energies.

* *E-mail address*: tarasov@nscl.msu.edu

0375-9474/$ – see front matter
doi:10.1016/j.nuclphysa.2004.01.099

The last three features are clearly visible in Figure 1 where experimental and calculated spectra of ^{37}Cl and ^{37}S from the reaction ^{40}Ar(26.5 MeV/u) + ^{64}Ni are shown [2].

Various models have been developed for an explanation of these phenomena both theoretical, and empirical parameterizations. Some models are implemented in the LISE++ code. V.Borrel [4] et al. suggest that in the fragmentation process it is required the binding energy (B_n) of about 8 MeV per each nucleon has to be subtracted from the projectile energy:

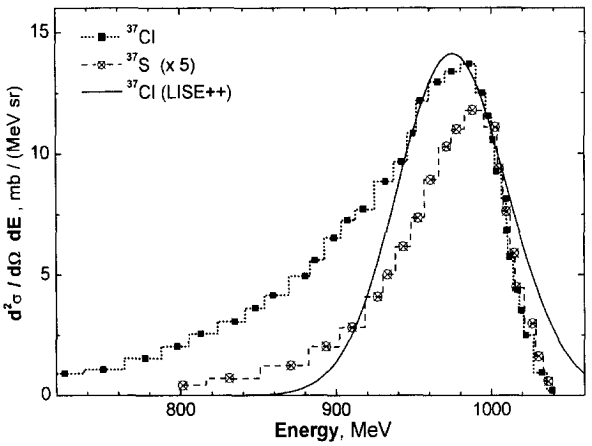

Fig. 1. Experimental energy spectra of ^{37}Cl and ^{37}S in the reaction ^{40}Ar(26.5)+ ^{64}Ni [2]. The spectrum calculated by LISE++ [3] for ^{37}Cl fragment assuming Goldhaber's model [1] and $\upsilon_F/\upsilon_P = 1$.

$$\upsilon_F/\upsilon_P = \sqrt{1 - B_n(A_P - A_F)/(A_F E_P)}, \tag{2}$$

where E_P is the projectile energy in MeV/u. If one assumes that the projectile becomes sheared in two, then several nucleon bonds have to be broken simultaneously. The number broken bonds can be treated as being proportional to the surface of contact [5]:

$$\upsilon_F/\upsilon_P = \sqrt{1 - 2E_S/(A_F E_P)}, \tag{3}$$

where E_S is the surface energy of contact and equal to $2\gamma S$, with γ denoting the nuclear surface tension coefficient (0.95 MeV/fm^2) and S is the area shared the abraded zone and the remaining fragment. Several models have been developed to describe the experimental widths of the fragment momentum distribution parallel to the beam. So for example a simple model suggested by D.Morrissey [6] predicts the width:

$$\sigma_{||} = 150\sqrt{A_P - A_F}/\sqrt{3}. \tag{4}$$

Friedman's model [7] relates the widths of distributions to the separation energies and an absorptive cutoff radius. Also Coulomb corrections have been incorporated in this work to explain the small values for the widths observed at lower energies.

Each of these models has advantages and disadvantages depending on energy region, projectile mass and other parameters. The new model "Universal parameterization" is developed and incorporated in the LISE++ program [3]. It is called "Universal parameterization" because it can reproduce the width of the momentum distribution, the ratio of fragment and projectile velocity as well as the low-momentum tail as function of the energy and thus accounts for the experimental observations not described within Goldhaber's model [1].

2. Universal parameterization

The Universal parameterization is based on the 3-step projectile fragmentation model. The first step is ***abrasion*** of projectile and formation of an excited prefragment. The shape of prefragment momentum distribution is assumed to be gaussian $\phi(p)$ following the statistical model. Exponential attenuation $\psi(p_1, p_2)$ is the next step resulting from ***friction*** due to kinetic energy loss, exchange of nucleons, and transformation into the internal degrees of freedom. With increasing projectile energy the contribution of friction decreases and at relativistic energies finally becomes negligible. In the third phase (***ablation***) the excited prefragment decays by emission of light particles and gamma-rays. A broadening of the velocity distribution characterizes the third step. The final momentum distribution $f(p)$ can be obtained by the convolution of the gaussian and exponential line shapes:

$$f(p) = \phi \otimes \psi \cong \exp\left(\frac{p}{\tau}\right) \cdot \left[1 - erf\left(\frac{p - p_0 + \sigma_{\mathrm{pf}}^2/\tau - s \cdot \tau}{\sqrt{2}\,\sigma_{\mathrm{pf}}}\right)\right], \tag{5}$$

$$\text{where } \tau = coef \cdot \sqrt{A_{PF} \cdot E_S}\,/\beta, \tag{6}$$

$$\text{and } \sigma_{\mathrm{pf}}^2 = \beta \sigma_{\mathrm{conv}}^2 \; A_{PF}(A_P - A_{PF})/(A_P - 1), \tag{7}$$

E_S is the energy needed to split the projectile, A_{PF} is the mass number of the prefragment, β is the projectile velocity, p_0 is the momentum of a final fragment corresponding to velocity of projectile (β), and σ_{conv}, s, $coef$ are parameters fit to data. Following [2,4] three different determinations of the separation energy are considered: a) mass differences between the projectile and the prefragment with nucleons cut off the projectile Q_g; b) surface energy excess S_E; c) the sum of first two $Q_g + S_E$. In order to establish parameters for all three possible separation energy methods 35 spectra in the energy region 26-2200 MeV/u were used from [2,4,5,8-12]. The fit values of the parameters σ_{conv}, s, $coef$ were determined assuming σ_{conv} to have the same value for all separation energy methods (see the results in Table 1).

The occurrence of a low-momentum tail in fragment momentum distributions at low projectile energies was addressed in a number of studies [4,5] and explained by an increasing contribution of transfer reactions. To estimate the contributions of various reaction mechanisms the energy spectrum was represented as the sum two gaussian distributions. The convolution model does not separate these reactions, and the final momentum distribution of the projectile fragmentation products includes the contribution of transfer reactions using the friction exponential attenuation.

The convolution model involves complex calculations and a numerical treatment is required. It is necessary to determine the most probable prefragment for each final fragment. Then the separation energy is

Table 1. Coefficients of the Universal parameterization depending on separation energy determination.

Energy separation method	σ_{conv}	$coef$	s
Mass difference (Q_g)	91.5	3.344	0.1581
Surface excess (S_E)		5.758	0.1487
Sum ($Q_g + S_E$)		2.936	0.1526

calculated using mass differences from tables or employing surface excess algorithm presented in [13]. The Universal parameterization is implemented in the LISE++ code [3] where all these intermediate steps are realized.

3. Comparison with experimental data

Recent experimental results [14] from RIKEN on the study of production cross sections and the momentum distribution of projectile fragmentation products in the reactions ^{40}Ar + Ta and ^{40}Ar + Be at 90 MeV per nucleon and the comparison with the models are presented in Figure 2. Differential cross section distributions were calculated with LISE++ normalized on the area of experimental spectrum. The sum of surface excess and mass difference was used for separation energy in the convolution method. Corrections for target thickness have been applied following [14].

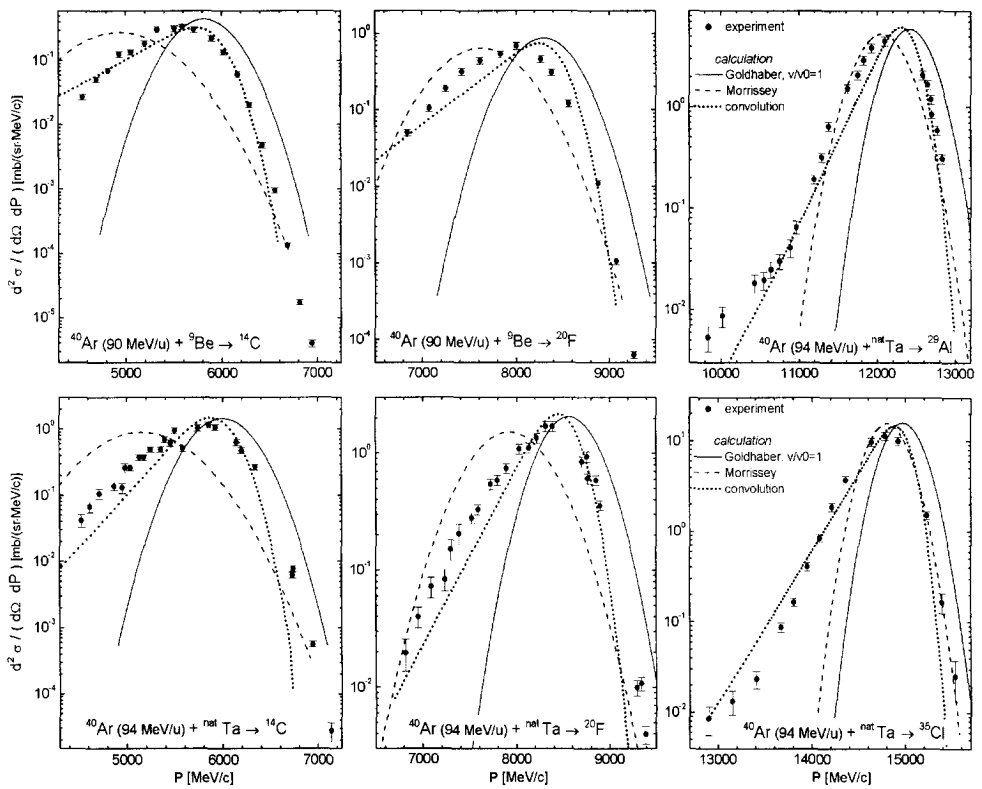

Fig. 2. Experimental spectra of ^{14}C, ^{20}F produced in ^{40}Ar + Be [14] and ^{14}C, ^{20}F, ^{29}Na, ^{29}Al, ^{35}Cl resulting from ^{40}Ar + Ta. Calculated spectra using Goldhaber's model [1] with fragment to projectile velocity ratio equal to 1 are indicated by solid lines. Dashed lines represents momentum distributions with widths and mean velocity based on Morrissey's systematics [6] and the convolution model calculations are shown by dotted lines.

4. Summary

The Universal parameterization basing on the 3-step projectile fragmentation model has been developed as a function of the projectile energy. This model can reproduce the width of the momentum distribution, the ratio of fragment and projectile velocity as well as the low-momentum tail. The Universal parameterization is implemented in LISE++ for fragment transmission calculations. It has been shown that the new experimental data in intermediate energies are found in good agreement with calculations done by the Universal parameterization.

References

[1] A.S.Goldhaber, Phys. Lett. B53 (1974) 306.
[2] M.C.Mermaz et al., Z.Phys. A324 (1986) 217.
[3] D.Bazin, M.Lewitowicz, O.Sorlin, O.Tarasov, Nucl.Instr. and Meth. A482 (2002) 314; http://dnr080.jinr.ru/lise and http://www.nscl.msu.edu/lise.
[4] V.Borrel et al., Z.Phys.A314 (1983) 191.
[5] F.Rami et al., Nucl. Phys. A444 (1985) 325.
[6] D.J.Morrissey, Phys. Rev. C39 (1989) 460
[7] W.A.Friedman, Phys. Rev. C27(1983) 569.
[8] Y.Blumenfeld et al., Nucl. Phys A455 (1986) 357.
[9] R.Dayras et al., Nucl. Phys. A460 (1986) 299.
[10] D.E.Greiner et al., Phys. Rev. Lett. 35 (1975) 152.
[11] J.Mougey et al., Phys. Lett. B105 (1981) 25.
[12] Y.P.Viyogi et al., Phys. Rev. Lett. 42 (1979) 33.
[13] J.Gosset et al., Phys. Rev. C16 (1977) 629.
[14] S.Momota et al., Nucl. Phys. A701 (2002) 150; M.Notani, PhD thesis, University of Tokyo (2001).